Innovative multifunctional finish for the improvement of Indoor Air Quality: Performance at laboratory and pilot scale

Innovative multifunctional finish for the improvement of Indoor Air Quality: performance at laboratory and pilot scale

Chiara Giosuè [a*], Natalia Czerwinska [a], Giada Remia [b], Francesca Stazi [a], Costanzo di Perna [b], Alessandra Mobili [a], Maria Letizia Ruello [a], Qaisar Maqbool [a,c], Francesca Tittarelli [a,d]

[a] Department of Science and Engineering of Matter, Environment and Urban Planning (SIMAU), Università Politecnica delle Marche, INSTM Research Unit, 60131, Ancona, Italy

[b] Department of Industrial Engineering and Mathematical Sciences (DIISM), Università Politecnica delle Marche, via Brecce Bianche 12, Ancona, 60121, Italy

[c] Institute of Material Chemistry, TU Wien, Getreidemarkt 9/BC, A-1060, Vienna, Austria

[d] ISAC-CNR, via Piero Gobetti 101, 40129, Bologna, Italy

*Correspondence to: c.giosue@staff.univpm.it

Graphical Abstract

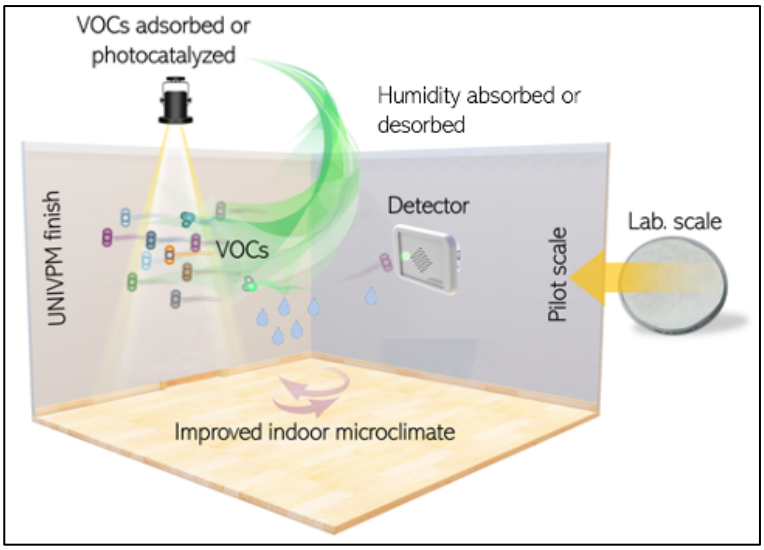

Abstract

In this study, the impact of an innovative multifunctional finish on the Indoor Air Quality (IAQ) in terms of temperature (T), relative humidity (RH), and volatile organic compounds (VOCs) was compared to that of a commercial finish for the same application as reference. The two finishes were applied on the same commercial substrate and tested both at laboratory and pilot scale. At laboratory scale, the water vapour permeability, the moisture buffering capacity and the depolluting activity by adsorption of the innovative finish was 15%, 100% and more than 200% higher than those of the commercial one on the same substrate, respectively. At pilot scale, the innovative finish was more effective than the commercial finish in buffering humidity variations (RH increases 53% slower compared to the commercial solution), temperature variations (-1.5°C), and decreasing VOCs concentration (from 14% up to 63%, depending to the test conditions). Therefore, the innovative multifunctional indoor finish has proven to be more effective than the commercial one in improving IAQ not only in laboratory but also at pilot scale.

Keywords

Indoor Finish, Indoor Air Quality (IAQ), De-polluting Properties, Moisture Buffering Capacity, Thermo-Hygrometric Properties, Pilot Scale Application.

Highlights:

- An innovative indoor finish was compared with a commercial one at lab and pilot scales
- The innovative finish was more effective to buffer humidity variations at lab and pilot scales
- The innovative finish had more depolluting abilities at lab and pilot scales
- The innovative finish is more effective in improving IAQ at lab and pilot scales

1. Introduction

Due to lifestyle changes people spend up to 90% of their daytime indoors in confined environments, such as houses, schools, offices, shopping centres, gyms, etc. [1]. Since the 2030 Agenda for Sustainable Development highlighted that all productive sectors should contribute to the reduction of greenhouse gasses (GHGs) emissions [2] and 40% of the global CO_2 equivalent emissions are produced by the construction sector [3] the current tendency is to provide more tightly sealed construction to create a stable internal environment that retains heat, thus leading to energy conservation.

However, the 13th goal of the 2030 Agenda "Climate Action" includes green and Nearly Zero Energy Buildings (NZEB) able not only to save energy and water, and reduce CO_2 emissions, but also to improve occupants' health and well-being. But passive and near-zero energy projects use building materials with high thermal inertia and limit the implementation of Heating Ventilation Air Conditioning (HVAC) systems. Consequently, the air circulation needed to maintain a good indoor air quality (IAQ) for a healthy environment may be impeded which can affect the comfort of occupants. The increase of Volatile Organic Compounds (VOCs), moulds, airborne particles and inadequate relative humidity (RH) levels [4] [5] affects the comfort and health of occupants with both short- and long-term effects such as the well-known Sick Building Syndrome (SBS), a disease caused by poor-quality ventilation, recognized by the US National Institute for Occupational Safety and Health (NIOSH) [6] .

The need for more comfortable and healthier environments in combination with efficient buildings requires new approaches such as the development of passive systems that can assist the active ones, such as air conditioners, purifiers, or dehumidifiers, currently used to improve IAQ [7] [8]. In this context, finishes covering the surface of internal walls and ceilings, thanks to their high surface area exposed to indoor environment, can play an important role in passively improving IAQ [9] [10] [11] [12]. In finishes for indoor applications, highly porous materials have been demonstrated able to act both as RH buffers and as depolluting system to decrease VOCs concentrations. In this regard, it has already been confirmed that moisture transport, storage, and pollutants removal (for example toluene) is influenced by porous building materials [13] [14].

Concerning the depollution abilities of materials, adsorption is the most effective process whereby a gas or a liquid (adsorbate) is passively removed from an air stream/atmosphere or fluid and transferred to the solid surface of an adsorbent [15]. Consequently, to achieve high efficiency, adsorbent materials should have a large specific surface area (approximately 300-3000 m^2/g) to assure a high solid-fluid contact area [16]. In depolluting processes, adsorption is often combined with another superficial phenomenon known as Heterogeneous Photocatalytic Oxidation (PCO) [17] [18] [19] [20]. In PCO, under radiation (mainly UV), reactive radicals from ambient O_2 and H_2O react with VOCs due to activated catalytic semiconductors such as titanium dioxide (TiO_2). These additives can be incorporated either in bulk or applied as a coating on the finishes to mineralize the adsorbed pollutants into less harmful substances [21] [22]. Hydraulic lime (HL)-based products generally have higher depolluting properties than cement-based ones [23] due to the higher presence of micro-pores and fewer nano-pores (gel pores) in the matrix which may hide the catalytic sites [24] [25] [26] [27]. Indeed, in case of bulk addition of TiO_2, the PCO activities are significantly affected by macro/micro pores and components of the finish [21] [22]. HL is also a more sustainable binder than cement since its production has a lower energy impact [28]. Moreover, free-lime (CaO) which is part of HL composition, can capture CO_2 (associated with greenhouse gases) by carbonation during the setting and hardening of the binder, thus contributing to a more favorable CO_2 balance [29]. Sustainability and reduction of indirect CO_2 can also be guaranteed including wastes or by-products in the binder or as aggregates [30] [31] [32] [33].

Concerning indoor humidity control by materials, indoor finishes with high water vapour permeability and Moisture Buffering Capacity (MBC) [34] can guarantee the indoor optimal RH ranges [35] of about 40% [36]. Earth plasters have a greater effect on the hygrothermal balance if compared to air lime, gypsum, and cement plasters [37]. Many laboratory-scale studies aimed at improving IAQ by means of adsorption/PCO in paints, plasters and finishes have been reported in the literature [38], including real scale experimental analysis [39] [40].Vega-Mendoza et al. tested the self-cleaning and CO_2 remediation of an alkali-activated fly ash photocatalytic mortar coating incorporating α/β-Bi_2O_3 homojunctions as a photocatalyst with high visible-light response [41] in a batch reactor. Jeon et al. focused on the improvement of IAQ by using a toluene adsorption paint with activated carbon in an inorganic binder both in laboratory static conditions and in an urban residential apartment [42]. A photocatalytic TiO_2-based paint was also tested to decrease NO_2 concentrations in a lecture room of the Technical University of Madrid [43].

Some of the present authors have proposed an innovative inorganic finish (Patent IT 102017000033750 – Multifunctional Mortar) which has been demonstrated to improve IAQ in terms of MBC and depolluting ability at laboratory scale [44] [45] [46]. In the patented mix, depolluting abilities are enhanced by coupling unconventional adsorbent aggregates to photocatalytic TiO_2 particles. The use of adsorbents currently not employed in construction, but in chromatographic techniques and filters for water and air purification, allows to increase lightness, permeability to water vapour and buffer properties of the finish. HL and non-hazardous special wastes, such as fly and bottom biomass ashes, not only ensure good mechanical properties but also the environmental sustainability of the product. However, it is well known that the results obtained at the

laboratory scale may be overestimated [47] [48] and have no practical relevance when moving to real scale. Also, the influence on thermo-hygrometric properties of the whole wall package [49] is of utmost importance [50] , since finishes are applied on indoor surfaces.

Recent literature shows a limited number of studies that demonstrate passive VOCs removal by mortars relying on the combined exploitation of adsorbing and photocatalytic properties of the innermost surface of the building envelope. In fact, generally literature studies have been carried out at laboratory scale and for outdoor applications; in some cases, the reproduction of the real environment was done through modeling [51]. Moreover, the depolluting materials tested in real environments [38] are commonly incorporated into building components (i.e. ceilings, flooring, plasters or plasterboards) rather than in finishing materials. Finally, to the best of the authors' knowledge, there are no previous works based on the comparison of multiple properties such as thermo-hygrometric and depolluting ones in on-site applications.

Therefore, the aim of this paper is to investigate the properties of the multifunctional innovative finish mix compared to a commercial one, both at laboratory and pilot scales. Both the patented and commercial finishes were applied on the same commercial substrate and compared in terms of thermo-hygrometric and depolluting properties in lab scale tests. Then in pilot scale tests, the patented finish and the commercial reference were applied on the same commercial substrate in two different dedicated test boxes under the same environmental conditions. The indoor parameters, such as Temperature (T), VOCs concentration and RH, of the boxes were compared to verify the benefits given by the multifunctional finish to IAQ.

2. *Materials*

The innovative finish (labelled "U" in the following text) was prepared with a commercial natural hydraulic lime (NHL), a mix of adsorbent materials and special wastes for aggregates, TiO_2 filler and commercial admixtures.

The commercial NHL was the product i.pro CALIX BLANCA NHL 3,5 (Heidelberg Materials – Italcementi) according to the standard UNI EN 459-1, with a declared density of 2700-3000 kg/m^3.

The selected aggregates were a mix of adsorbent materials not commonly used in the construction sector, and fly/bottom ashes from the thermal treatment of biomasses. The adsorbent aggregate had a water absorption capacity to reach the saturated surface dry (ssd) condition of 86%, a density of 1310 kg/m^3 and a maximum grain size diameter (D_{max}) of 300 μm. The biomass ashes came from an Italian biomass-to-energy valorisation plant, located in Rieti (Lazio region). The water absorption capacity was 49% and 20%, the ssd density was 1410 and 1940 kg/m^3 and D_{max} was 1000 and 210 μm, for the bottom and fly ashes, respectively [52].

Aeroxide® by Evonik, with nano-size particles of 20–50 nm, was chosen as TiO_2 photocatalytic addition. The specific surface area was 52 m^2/g, the micropore area 0.36 m^2/g and the average pore diameter (4V/A) 146 Å, as measured by BET (Gemini 2360 Surface Area Analyzer equipped with FlowPrep 060, micrometrics). The pH of a 4% water dispersion was 3.5–4.5, and the density was 3.1 g/cm^3 as declared in the technical datasheet. The amount of TiO_2 added to the finish was 2% of total powder mass.

To optimize the fresh properties, facilitate the application, and avoid shrinkage cracking after the application on the substrate, 3 commercial admixtures were added to the patented mix when applied at pilot scale: i) shrinkage reducing admixtures (SRA) at 0.5% of total powder mass; ii) micro cellulose at 0.7% of total powder mass and iii) superplasticizer at 0.02% of total powder mass.

The U finish was prepared by adding water until a proper workability for the application was reached (measured as indicated in section 3.2.), which was about 40% of the total weight of powders. It was applied on the commercial substrate in two layers for a total thickness of 3 ± 0.5 mm.

The properties of the U finish were compared to those of a commercial one, limepaint by Diasen® (labelled "L" in the following text), used as a reference. L is a water-based paint currently used as a ready-to-use finish for lime-based materials that can be applied on walls, renders, and ceilings.

Calce Storica by Diasen® (C), was selected as commercial substrate for the application of both L and U finish. C is a premixed mortar composed by commercial aggregates and natural hydraulic lime as binder, prepared by adding 18% of water, as indicated in the technical datasheet. The two finishes were applied after 15 days of curing: at lab scale, curing was performed at T of 20 ± 2 °C and RH of 60 ± 5%, while at pilot scale at room conditions with T ranging from 18 to 20 ± 2°C and RH from 80 to 60 ± 5%.

For on-site applications, the commercial substrate C was applied for 20 mm on the entire wall for 2 cm. Then, the U finish was applied in 2 consecutive layers, approximately 1.5 mm thick each, and TiO_2 was added only in the finish of the outermost layer. Following the technical datasheet, a layer of fixative (D20 supplied by Diasen®) was applied before the L finish. The labels and descriptions of all tested materials are reported in Table 1.

Table 1 label and description of materials

Label	Description
U	Innovative finish: a hydraulic lime-based finish with adsorbent materials, industrial by-products, TiO_2 filler and commercial admixtures
L	Commercial finish: ready-to-use lime-based water paint
C	Commercial base coat: premixed hydraulic lime-based mortar
C-U	Finish U applied on base coat C
C-L	Finish L applied on base coat C

3. Laboratory tests methods

The full characterization of the innovative multifunctional finish (U) in terms of mechanical, thermo-hygrometric, mould growth inhibition and depolluting properties, has been recently published [44].

The ***mineralogical composition*** of the ashes was investigated by X-ray analysis, using a RX Philips PW 1730 X-ray diffractometer (operating voltage/current 40 kV/30 mA; scan mode: continuous speed, 3°/min). The main components were quantified through TGA (Metter Toledo) at speed rate of 10 °C/min under oxidizing atmosphere.

168 The ***workability*** was evaluated by slump test according to the UNI EN 1015-3:2007 standard and resulted in a
169 stiff consistency, as classified in UNI EN 1015-6:2007.
170 ***The compressive strength*** test was carried out according to UNI EN 1015-11:2007 on three 4 × 4 × 16 cm
171 specimens by means of a hydraulic press (Galbaldini - Cardano al Campo (VA) Italy) with a precision of 1%
172 and the average results have been reported.
173 The ***thermo-hygrometric properties*** were evaluated on three specimens for each mix, and the average values
174 reported.
175 The thermal conductivity (λ) of C-L and C-UNI was measured at T = 20 ± 2 °C and RH = 50 ± 5% according
176 to UNI EN 12664:2002, following equation (1):
177 $$\lambda = \frac{Q \cdot s}{A \cdot (T_2 - T_1)} \quad (1)$$
178 where Q/A is the heat flux (W/m^2), s is the sample thickness (m), and T_1 and T_2 (K) are the temperatures at the
179 two different sides of the sample, set at 15 °C and 30 °C.
180 The hygrometric properties were evaluated both in static and dynamic conditions, in terms of water vapour
181 resistance factor (μ) and Moisture Buffering Value (MBV), respectively.
182 The water vapour permeability was tested according to the UNI EN 1015–19:2007, and data were processed
183 according to the UNI EN ISO 12572:2007 standard, which evaluates the μ value of cylindrical specimens (h =
184 3 cm, d = 20 cm). The tested specimens were C-L, C-U and C.
185 The MBV defines the humidity absorbed and desorbed by the material on the surface unit when it is placed in
186 an environment at RH of 75% for 8 hours and of 33% for 16 hours, according to a simplified procedure of
187 NORDTEST, which evaluates the MBC of the material [53] [54] [55]. For each type of specimen (C, C-L, and
188 C-U), for each specimen the average MBV calculated over 3 cycles was obtained. The tested specimens were
189 cylindrical (h = 3 cm, d = 10 cm) with the lateral surface previously sealed with silicone to guarantee a
190 homogeneous water vapour flow.
191 The ***depolluting properties*** of the finishes were tested on cylindrical specimens (h = 0.8 cm, d = 8 cm) in terms
192 of adsorption and photocatalytic activity [46].
193 The adsorptive properties were evaluated by a batch test where Methyl Ethyl Ketone (MEK) was used as a
194 model pollutant. The specimen was placed in a glass box of 17 l, with a fan on the bottom, and 50 μl of MEK
195 was injected with a micro-syringe from the upper hole hermetically closed with a rubber sept, to obtain inside
196 the box a theoretical initial MEK concentration of 797 ppm. The MEK concentration inside the box in time
197 was evaluated by collecting 10 μl of air every 8 mins for 90 mins and analysing MEK concentration by a gas
198 chromatograph (Carlo Erba Gas 8000 Top; Flame Ionization Detector; injector split 1:15; carrier flow 2
199 ml/min; capillary column, 25 m × 0.32 mm, 0.52 μm cross-linked methyl siloxane; isotherm condition 40 °C).
200 The photocatalytic activity was assessed according to the UNI 11247:2009 standard, which measures the
201 nitrogen oxides (NOx) degradation rate in plug flow condition. C-L and C-U were tested both under VIS
202 (Philips lamp, 42W) with intensity equal to 9 ± 1 W/m^2 as detected by Delta Ohm HD 2101.1 photo radiometer
203 (probe LP471 RAD 400 – 1050 nm), and UV radiation (halogen lamp, 400W) with measured light intensity
204 of 20 ± 1 W/m^2 (probe LP471 UVA 315 – 400 nm). The NOx flux was supplied by a NOx tank (SAPIO S.r.l.,

Monza, Italy), for a concentration of 500 ± 5 ppb in a dilution flow of 1.5 l/min, and was kept constant by mixing with air at T = 25 °C and RH 50 ± 10% using a dilution system (Calibrator 8188, Rancon Instruments S.p.A., Milan, Italy) continuously monitored in terms of NOx and NO concentrations by a chemiluminescence NOx analyser (nitrogen oxide analyser model 8841; Monitor Labs, Englewood, CO, United States). Each tested specimen was placed in a 3 l borosilicate reactor and, as soon as the NOx flux was stable, photocatalytic activity (%D) was evaluated following equation (2):

$$\%D = \frac{C(dark)-C(light)}{C(dark)}100\% \quad (2)$$

where %D is the percentage of degradation and C(dark) and C(light) are the concentrations of NO or NOx in the dark and light conditions (after 10 min of irradiation), respectively.

4. On-site experimental methods

For on-site monitoring, a test room has been set up (Figure 1). The area identified for the experimentation is located in Ancona, central Italy (latitude: 43.54°, longitude: 13.37°, altitude: 137 m). The experiment was conducted in a prefabricated test room, measuring approximately 3 x 3 x 3 m^3 characterized by an aluminum sandwich panel envelope with an internal layer of mineral wool 12 cm thick.

On the north-eastern and western sides, a further 10 cm thick external insulation layer of polystyrene with an aluminum finish gave the walls a total thickness of 22 cm. On the southern side, the insulation layer thickness was 12 cm and, externally, a white rendered cement board was inserted, reaching a total thickness of 15 cm.

The internal volume was divided in half: an antechamber hosting the computer for monitoring and a room on the southern exposure, which was in turn divided into two sub-rooms BOX1 and BOX2, (each with dimension of 1.2 x 1.2 x 2.9 m^3), hosting on the internal wall facing south the innovative C-U finish and the commercial C-L finish, respectively.

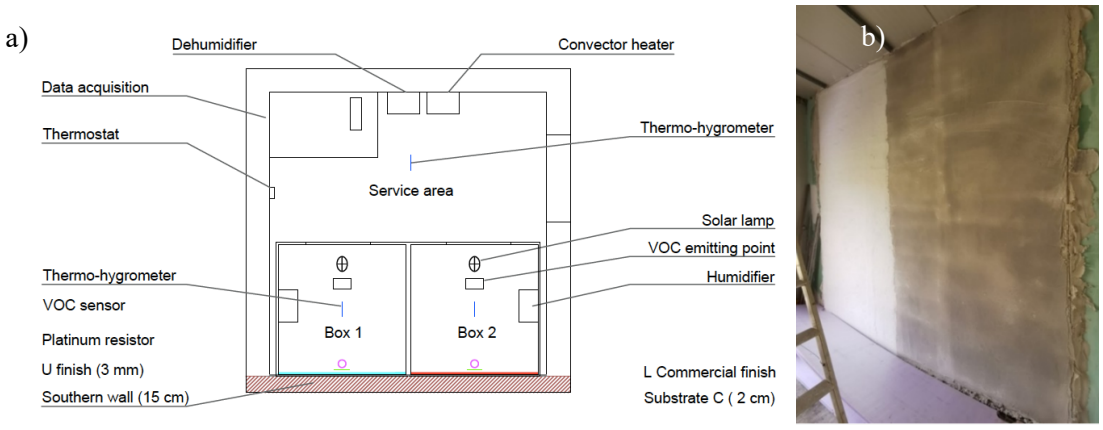

Figure 1. a) Plan of the experimental room and b) image of the two finishes before the test room separation

The two test boxes were closed with plasterboard panels and sealed with adhesive tape. A data acquisition and remote microclimatic control system was set up outside the two boxes, in the service area. The system provided the continuous data acquisition of: i) VOCs concentration inside box 1 and box 2 (VOC1, VOC2), ii) Air Temperature inside box 1 and box 2 (T1, T2), iii) Surface Temperature of the two finishes (RTD1, RTD2), iv)

Air Temperature of the service area (Tser), v) Relative Humidity inside box 1 and box 2 (RH1, RH2) and Relative Humidity of the service area (RHser). Inside each box, the irradiance was measured before the beginning of the tests to assess the photocatalytic properties of the finish. Table 2 provides the information about the sensors.

Table 2. List of the sensors used in the experiment.

Parameter	Sensor type	Model	Range	Accuracy	Area of installation
Air temperature	Thermo-hygrometer	PCMini52, Michell	-20 °C to 80 °C	± 0.2 °C	Service area Test area
Surface temperature	Platinum resistor	PT100	-40 °C to 80 °C	± 0.05 °C	Test area
Relative humidity	Thermo-hygrometer	PCMini52, Michell	0 to 100%	<±2%	Service area Test area
VOCs concentration	Photoionization detector - PID	Series 900, Aeroqual	0 to 30 ppm	±0.02 ppm +10%	Test area
Irradiance	Photo-radiometer	HD 2102.2, DeltaOhm (Probes LP471UVA, LP471RAD)	0.1 mW/m^2 to 2000 W/m^2	±1digit	Test area, only for the test of irradiance

In the service area, a control system based on LABVIEW allowed to maintain constant within the two boxes RH and T values = 55 ± 5%, and 20 ± 0.5 °C, respectively.

Inside each box a humidifier (Medisana, model V-401671, 4.2 l capacity) and two different sources of radiation (lamps), namely a solar lamp (Ultravita LUX Osram, 300W) and a UV lamp (RepTech 100W), were installed. The measured irradiances were 3 and 8 W/m^2 in case of UV radiation and 18 and 30 W/m^2 in case of VIS radiation for the solar lamp and the UV lamp, respectively. When necessary, inside each box a MEK emitting point was placed to act as an internal source of VOCs.

To wait for proper curing of materials, the data acquisition of the environmental parameters of the two boxes started one month after the application of the finishes.

The following conditions were explored:

• **Temperature increase:** from 20 to 28 °C by switching on the UV lamp with UV = 3 W/m^2 and VIS = 18 W/m^2. Tests were conducted in dark conditions and under UV/VIS radiation provided by the UV lamp, to evaluate the possible photocatalytic activity. The irradiance of UV/VIS measured by a photo-radiometer on the surface of the pilot wall, perpendicularly to the lamp, was equal to 8 W/m^2 and 30 W/m^2, respectively.

• **RH increase:** by switching on the humidifier.

• **VOCs concentration change:** by MEK (used as a model pollutant) static or spot load or by UV lamp switched on. For the static load test a beaker with 10 ml of MEK was placed in the center of each box floor; for the spot load test, 10 µl and 50 µl of MEK was injected inside each box by a graduated syringe.

5. Laboratory test results

5.1. Preliminary evaluations on ashes composition and physical-mechanical properties of the innovative finish

The mineralogical composition of ashes was characterized by X-ray diffraction analysis (Figure 2). The main detected compounds were calcium carbonate ($CaCO_3$), quartz (SiO_2), calcium oxide (CaO) and Portlandite ($Ca(OH)_2$); the last two calcium-based compounds can contribute to the binding phase. As crystalline species, traces of magnesium oxide (MgO) and sylvite (KCl) were also detected but the low concentration of the latter is confirmed by the absence of efflorescence on the surface of the prepared specimens.

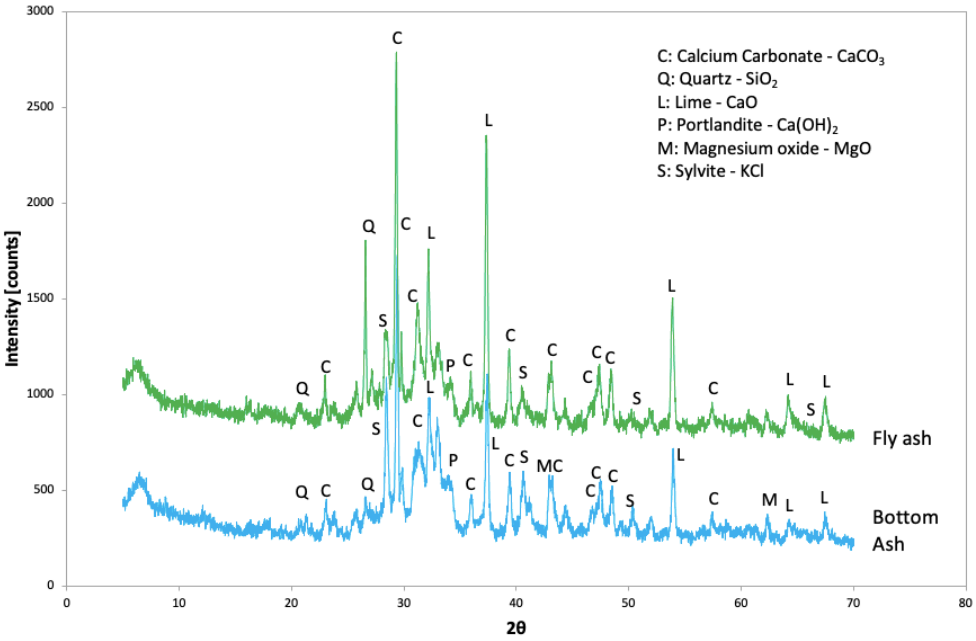

Figure 2. XRD analysis of fly and bottom ashes.

TGA quantified the main components of the biomass ashes (Figure 3). The weight loss up to approximately 150 °C through an endothermic process is correlated to the loss of un-bound H_2O. The exothermic process from approximately 120 to 450 °C is due to the combustion of organic material; the unburnt organic carbon with a related exothermic reaction at T around 400-450 °C is detected only in fly ash. From 470 to 550 °C the endothermic weight loss is due to the decomposition of $Ca(OH)_2$ whereas the final endothermic weight loss up to about 800 °C is due to the decomposition of $CaCO_3$, quantified as 25.4% and 30.0% of the total content for fly and bottom ashes, respectively. $Ca(OH)_2$ is more present in fly ash than in bottom ash, with contents of 8.2% and 0.8%, respectively.

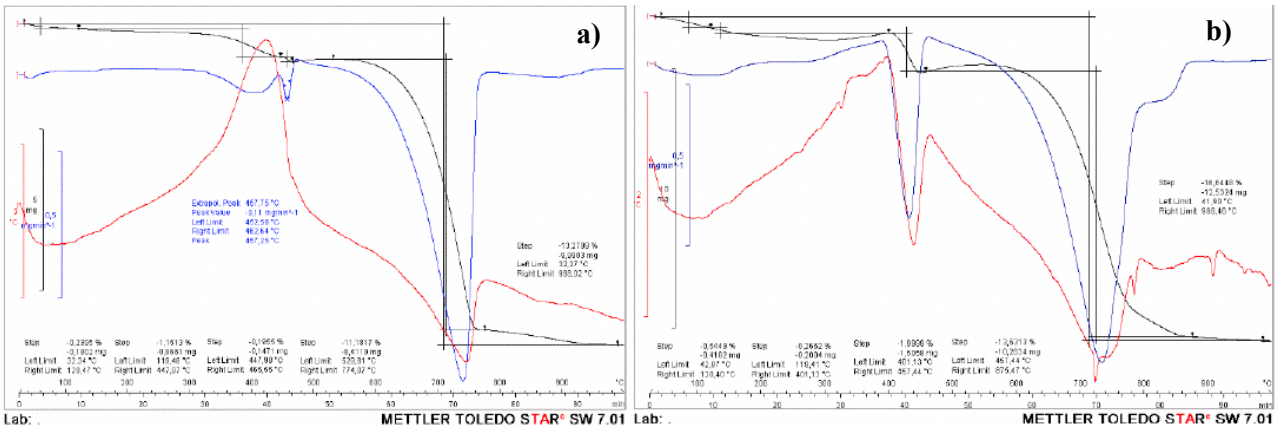

Figure 3. TG/DTA of fly (a) and bottom (b) ashes.

The workability of the U finish was evaluated through the slump test and resulted in a stiff consistency, as classified in the UNI EN 1015-6:2007 standard.

The compressive strength of U finish was 8.7 MPa, a higher value compared to that generally obtained by a 3.5 NHL-based mortar, probably due to calcium-based compounds such as CaO and $Ca(OH)_2$ in the added ashes which contribute to the binding phase.

5.2 Thermo-hygrometric properties of studied mortars and systems

The thermal conductivity values for C (substrate), C-L and C-U were: 0.112, 0.119 and 0.123 W/mK, respectively. As expected, the presence of a finish, regardless if commercial or innovative, had a negligible effect on λ value: indeed, the C-U system had less than 5% higher thermal conductivity than C-L and C.

The μ value was 21 for C-L and 18 for C-U demonstrating that the water vapour permeability is mainly affected by the substrate C ($\mu = 19$).

The MBV values were 0.26, 0.15 and 0.34 g/(% m^2) for C, C-L and C-U, respectively; this means an increase of the hygroscopic buffer capacity of more than double when the innovative U finish is applied.

5.3 Depolluting properties

As regards depolluting properties, the results are presented in terms of Ci/C0 percent where C0 is the theoretical initial concentration of MEK in the box and Ci is the concentration in the box during the air sampling. After 90 mins of testing, C-L presented an adsorption capacity of 19% while C-U of 56%.

The photocatalytic activity under UV radiation was detected only in C-U specimen with TiO_2, and degradations of NO and NOx of 28% and 25% were measured, respectively. In case of C-L, no degradation was detected as expected due to the absence of a photocatalytic agent [46]. The results are shown in Table 3.

Table 3. Summary of the results obtained by lab scale tests

Parameter		**C**	**C-L**	**C-U**
Thermal conductivity, λ	W/(mK)	0.112	0.119	0.123
Water vapour resistance factor, μ	-	19	21	18

Moisture Buffering Value (MBV)	g/(% m^2)	0.26	0.15	0.34
Adsorption capacity (MEK)	%	-	19	56
Photocatalytic degradation of NO	%	-	0	28
Photocatalytic degradation of NOx	%	-	0	25

306

307 ## 6. *On-site tests results*

308 ### *6.1. Comparison under free running conditions*

309 T and RH values recorded one month after the application of finishes in the two boxes are shown in Figure 4,
310 the typical conditions with no external changing. The box with the U finish always showed approximately 5%
311 higher RH (named RH1 in the figure) than traditional L finish (RH2), probably due to the higher water content
312 of the U-finish. In the two boxes, the T values were similar (20 ± 1 °C) at night and during the non-central
313 hours of the day. On the other hand, in the warmest hours of the day (from 11:00 AM to 4:00 PM), the
314 innovative finish revealed slightly reduced T peaks with a more flattened trend and maximum achieved
315 temperature levels around 0.5 °C lower than C-L, indicating a greater thermal inertia.

316

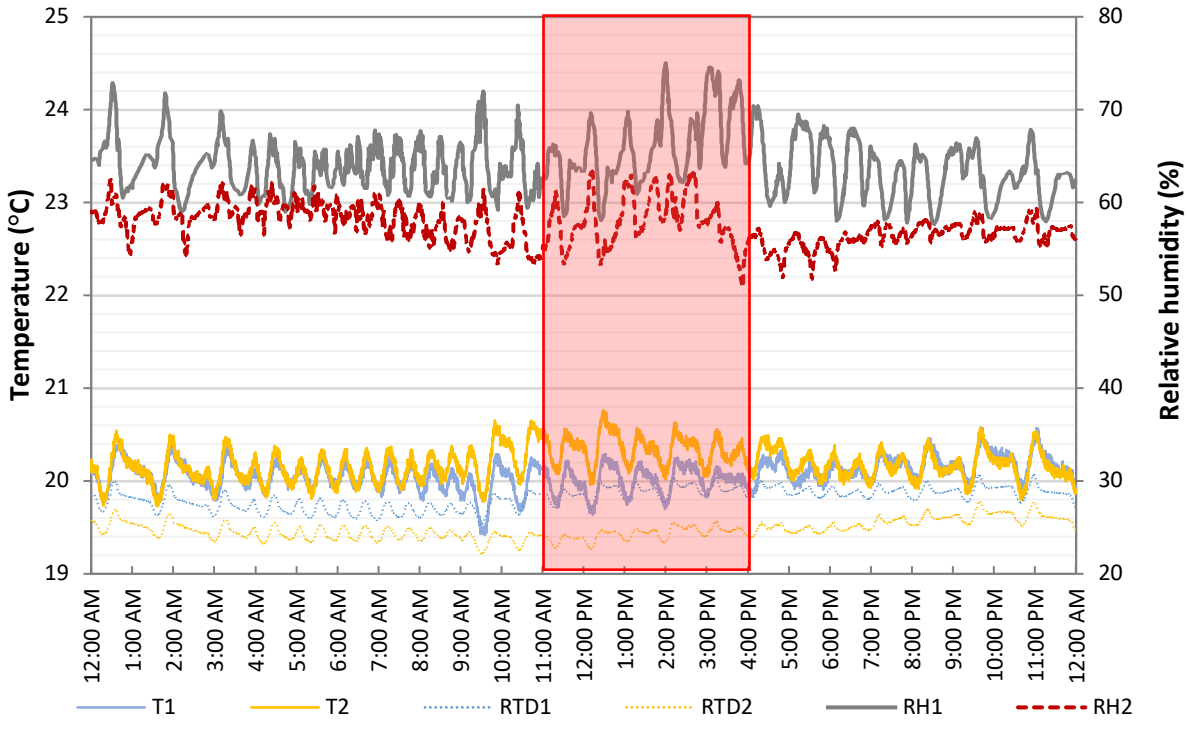

317

318 Figure 4. Initial conditions: 24 hours of monitoring of the two boxes (day 10 of monitoring). The warmest hours are
319 highlighted. The number 1 is for box 1 (C-U) and number 2 for reference box 2 (C-L).

320

321 Figure 5 shows the average VOCs concentration recorded for two selected weeks of the monitored period.
322 During the first week, up to 70% higher concentration of VOCs was observed in the box with the commercial

L finish compared to the one with the U finish. After this period, the VOCs concentration recorded in the box with C-L reached an average daily value from 0.40 ppm to 0.30 ppm, while in the box with C-U from 0.20 ppm to 0.15 ppm. This can be attributed both to the lower VOCs emissions of the U finish compared to the L finish and to the higher VOCs adsorption capabilities of the U finish compared to the commercial L finish.

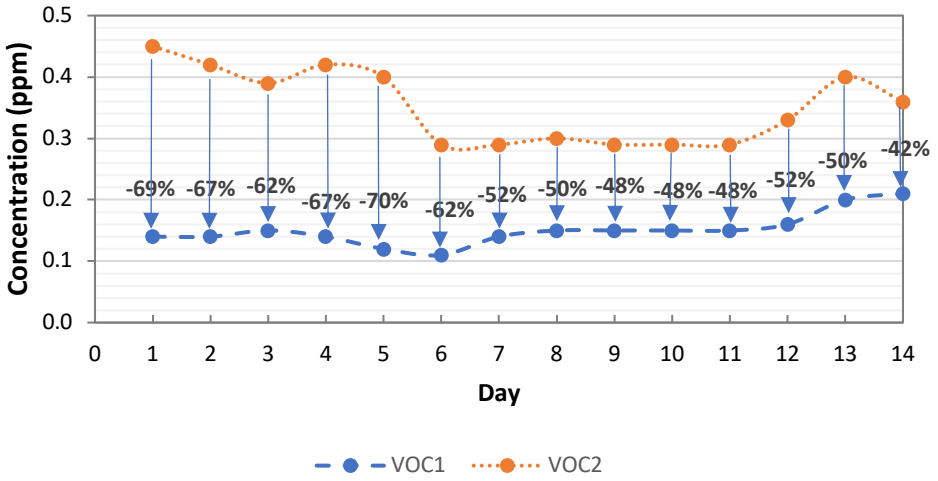

Figure 5. Initial monitoring period (14 days): initial VOCs concentration detected in box1 and box 2. The number 1 is for box 1 (C-U) and number 2 for reference box 2 (C-L).

6.2. Comparison under high indoor temperatures

Figures shows the results obtained by increasing the indoor temperature from 20 °C to 28 °C, by turning on the solar lamp for 1 hour in each box to simulate warm days or household activities.

The rise of air temperatures in the two boxes (T1 and T2) was the same. However, 1 hour after the lamp turning off, T1 was slightly higher than T2 due to the higher thermal inertia provided by the U finish compared to the L finish. For the same reason, after switching on the lamps, the surface temperature of the U finish (RTD1) was approximately 0.5 °C lower than RTD2.

Figure 6 shows also the VOCs concentration variations with the temperature increase. In general, data showed an increase in VOCs released under higher temperature. After 1 hour of irradiation the VOCs concentration increased: inside box 1 with the new finish by 13% (from 0.27 ppm to 0.31 ppm); inside box 2 by 21% (from 0.43 ppm to 0.53 ppm), doubling the value obtained with the new finish.

Moreover, after turning off the lamp, in box 2 where the commercial finish was applied, VOCs concentration took 3 hours to return to a steady state value, 0.45 ppm instead of the initial 0.43 ppm. On the other hand, in box 1, VOCs concentration took only 1 hour to return to a steady state value, 0.27 ppm instead of initial 0.29 ppm.

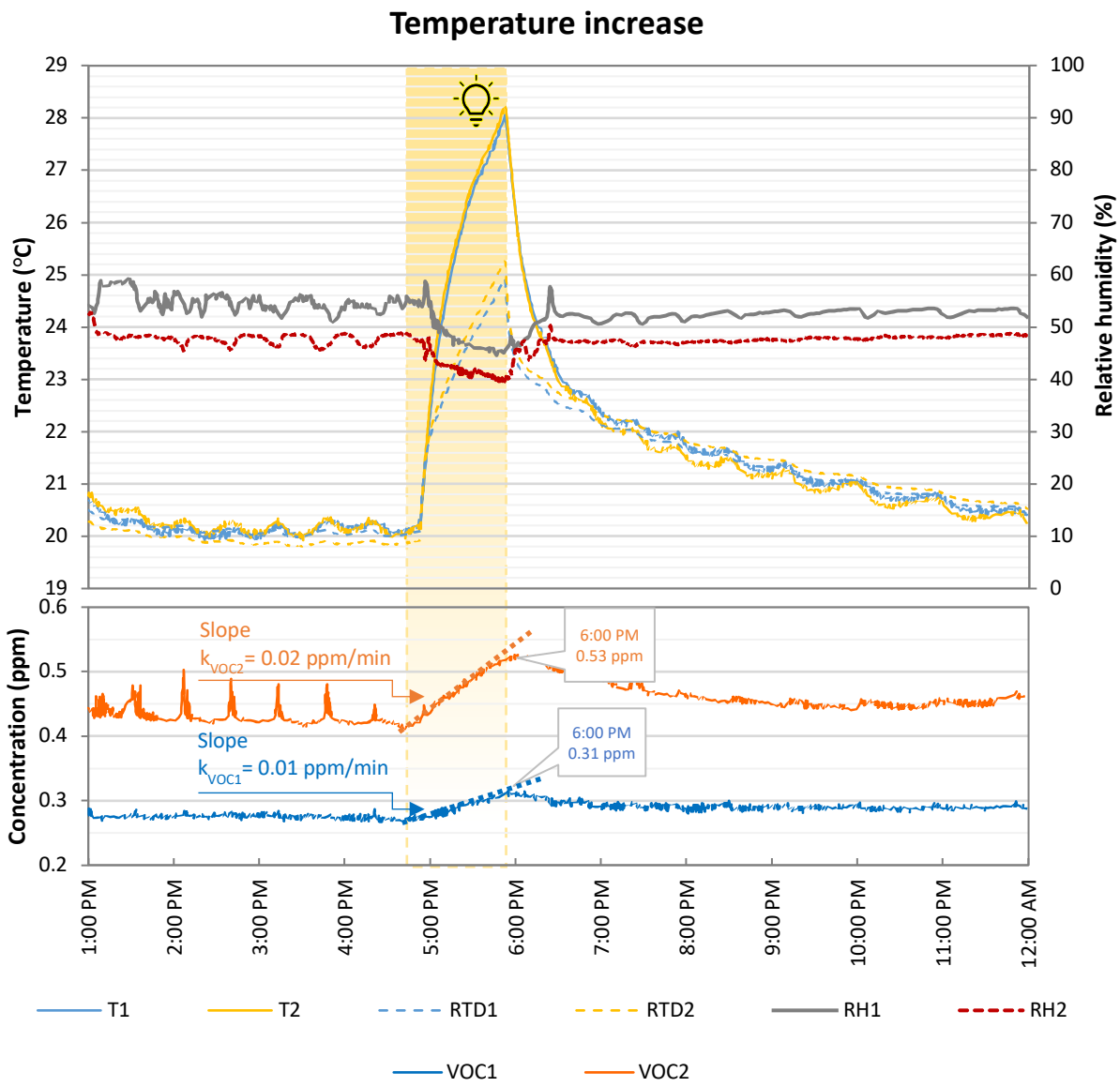

Figures 6 Comparison of the two boxes at the increase of temperature and increase of VOCs concentration due to T increase by irradiation. The number 1 is for box 1 (C-U) and number 2 for reference box 2 (C-L).

6.3. Comparison under high humidity regimes

Figure 7 shows the air temperatures and RH values recorded in the two boxes by increasing the relative humidity at 75% for 8 h to simulate the humid phase of the NORDTEST used in the lab scale. Since boundary conditions were the same in box 1 and box 2, the detected change was caused only by the different response of the finish to the high levels of humidity.

As soon as the humidifiers started working, the RH trend lines had different slopes: 0.15%/min for the reference C-L box 2 and 0.07%/min for C-U box 1, indicating faster RH increase in the box with the commercial products and a consequent lower moisture buffer ability. Moreover, when RH was set again at 50%, RH decreased faster in box 2 than in the reference box 1, demonstrating the higher hygrometric inertia of the innovative finish compared to the reference finish. The U finish provided the environment with a greater

thermal and hygrometric inertia by reducing the variations of T and RH, thus confirming the better ability of the innovative finish to behave as a thermal and hygrometric buffer compared to the commercial finish even at a pilot scale.

Figure 7 shows also the VOCs concentration changes due to RH changes. However, in C-L box 2, the VOCs concentration initially increased faster than in box 1, probably because MEK, adsorbed only superficially, was easily removed by water. Subsequently, the VOCs concentration remained quite stable and decreased very slowly due to natural decay. In case of C-U box 1, the VOCs concentration reached its maximum at a RH around 70% with values much higher than in box 2, probably because in presence of high RH values water saturated the porosity of the unconventional aggregates, causing the removal the high amount of MEK molecules already adsorbed during the load tests (desorption process).

Moreover, in both cases, the increase of VOCs concentration may be related to the competition between water and MEK molecules at the adsorption sites. The two spikes of VOCs concentration in box 1 and the high noise in VOCs concentrations trend in both boxes could be related to a possible interference between water drops generated by the humidifier and the VOCs sensor due to the relatively small volume of the box where the analysis is provided. In any case, this interference did not hide the evidence of VOCs desorption discussed above, demonstrating that environmental parameters such as T and RH also modify the response of finishes in terms of adsorption/absorption of airborne pollutants.

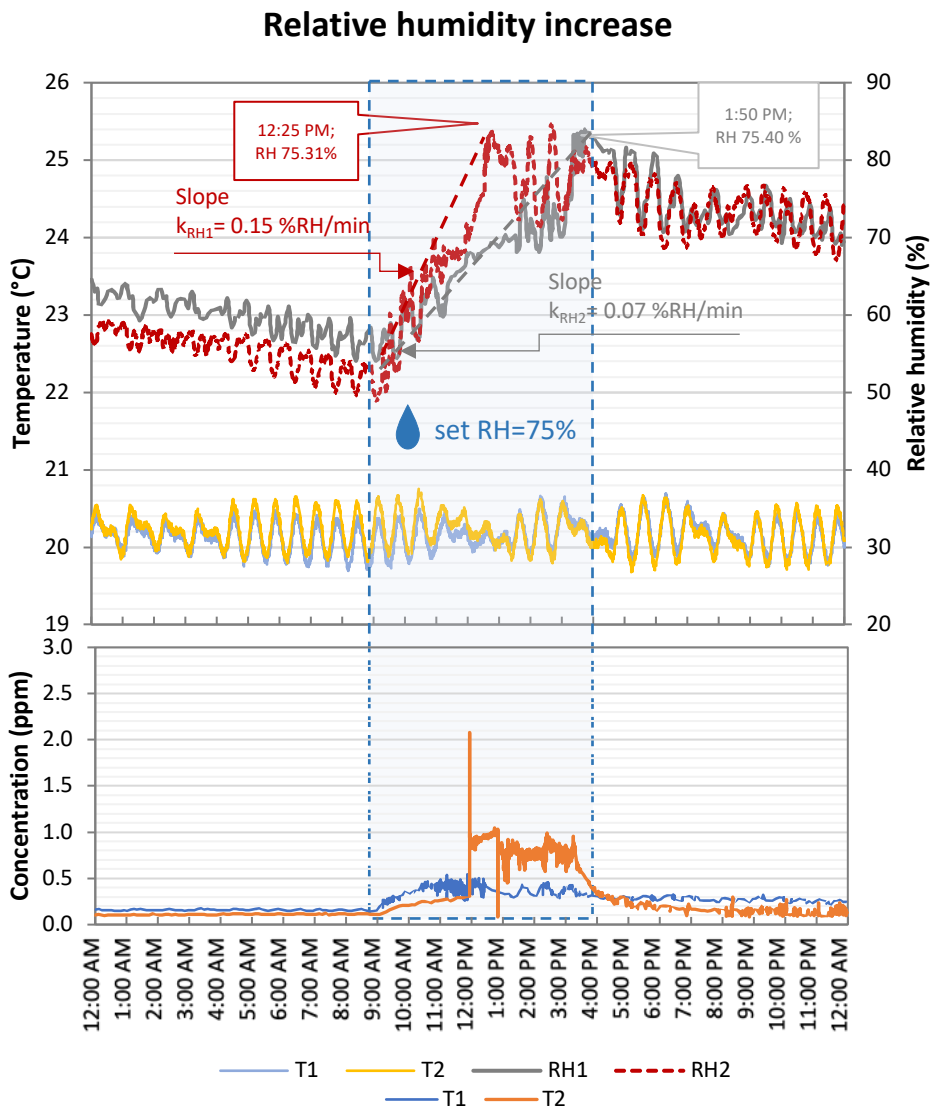

Figure 7. Comparison of the two boxes at the increase of temperature and VOCs concentration due to RH change; the number 1 is for box 1 (C-U) and number 2 for reference box 2 (C-L).

6.4. Comparison under high VOCs concentration

Figure 8 reports the environmental concentration of MEK after a static load. Before loading, in the two boxes VOCs were approximately 0.17 ppm. As soon as the MEK load a was inserted into the boxes, the VOCs sensors recorded an increase in concentration, followed by a steep slope and then a stationary phase, meaning that an equilibrium condition was reached. Although the values of the slopes of the initial phase were similar (0.06 ppm/min and 0.07 ppm/min for C-L and C-U, respectively), in the reference box 2 the MEK concentration increased up to 1.24 ppm, and then decreased very slowly in about 2.5 hours until stabilizing around approximately 0.39 pp. In box 1 with the new finish, the MEK concentration rose up to 0.94 ppm, and stabilized at 0.30 ppm, a lower value than that recorded in the reference box, confirming the depolluting ability of the innovative finish U. This demonstrates the natural concentration decay occurred in the two boxes and the passive adsorption property of the two materials, but also the greater depolluting efficacy of the innovative

finish U compared to L, since both the corresponding stabilization phase and the final concentration values were lower than the ones detected with L: at low concentrations, before loading, the curves coincided, but at high concentrations the U finish retained up to 20% more VOCs molecules than the reference L finish. Additionally, high concentration of VOCs implies high noise in both VOCs concentrations paths but more evident when C-L is applied since it was not able to adsorb as much MEK as C-U.

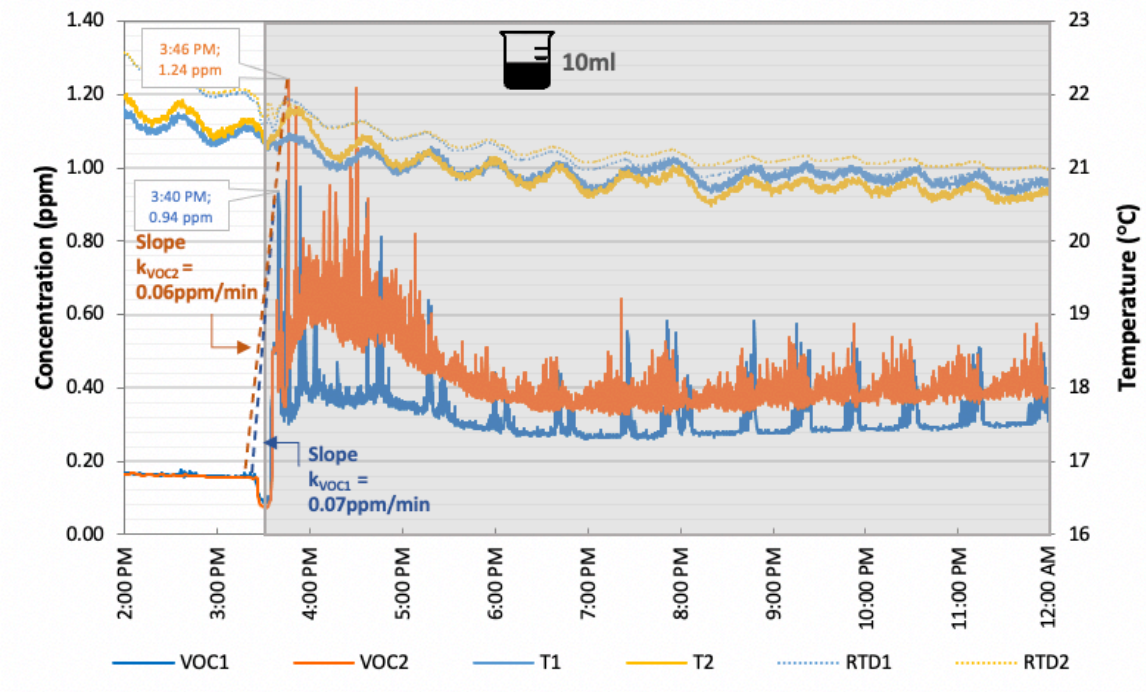

Figures 8. VOCs concentration and temperatures in the two boxes when static load of MEK was provided. The number 1 is for box 1 (C-U) and number 2 for reference box 2 (C-L).

Figure 9 shows the results obtained after the spot load of 50 µl MEK (corresponding to a vapour concentration equal to 2.7 ppm). The load was followed by a peak in VOCs concentration, with a maximum value of 5.77 ppm in box 1 and 6.70 ppm in the reference box 2. Subsequently, for the entire monitoring period, C-U maintained lower values of VOCs concentration compared to C-L in the box. The slopes of the decreasing phase of the spot load were equal to -2.78 ppm/min and -3.10 ppm/min for C-L and C-U, respectively.

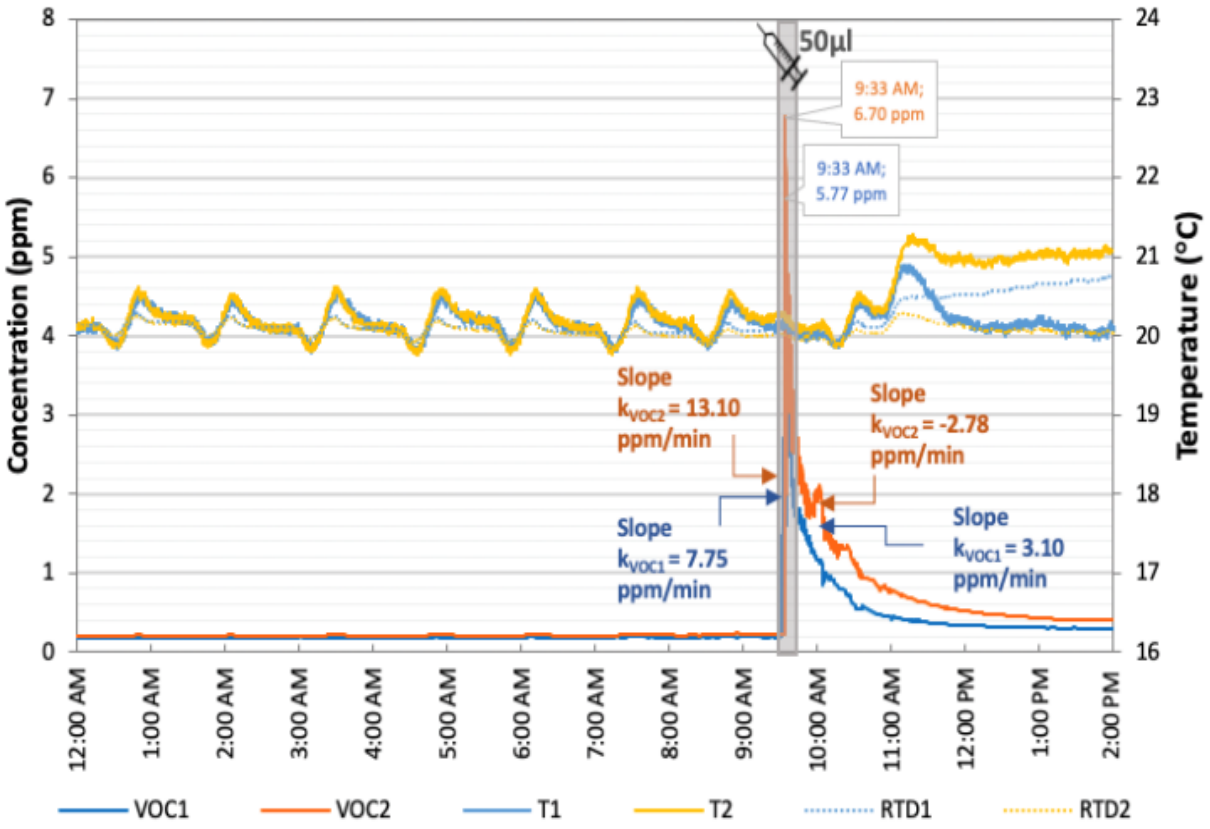

Figure 9. VOCs concentration and temperatures in the two boxes with spots loads of 50 µl of MEK in the test boxes. The number 1 is for box 1 (C-U) and number 2 for reference box 2 (C-L).

6.4. Comparison under high VOCs concentration and photocatalysis activation

Figure 10 shows the results obtained after the spot load of 100 µl MEK (corresponding to a vapour concentration equal to 5.3 ppm) and the activation of TiO_2 photocatalytic function by the UV lamp. The MEK load caused the occurrence of VOCs peaks in both boxes: 13.40 ppm and 4.98 ppm with a slope of 4.26 ppm/min for C-L and 0.52 ppm/min for C-U. Moreover, 30 mins after the spot load, the UV lamp was turned on for 1.5 h. During initial lighting, the VOCs concentration assumed divergent trends: in reference box 2 the L finish emitted VOCs +0.27 ppm for approximately 5 minutes, while in box 1 the U finish continued to adsorb pollutants, -0.26 ppm for the same time, with a difference in MEK concentration of 0.76 ppm between the two boxes. After 10 minutes of lighting, in reference box 2 the MEK concentration started to decrease again due to the natural decay of MEK. The depollution kinetics of the two combined processes (adsorption and photocatalysis) was also higher in C-U (0.05 ppm/min) than in C-L (-0.05 ppm/min). This means that in C-L only desorption and natural decay of MEK occurred, while in C-U also photocatalytic activity occurred, thanks to the presence of TiO_2, which decreased the VOCs concentration.

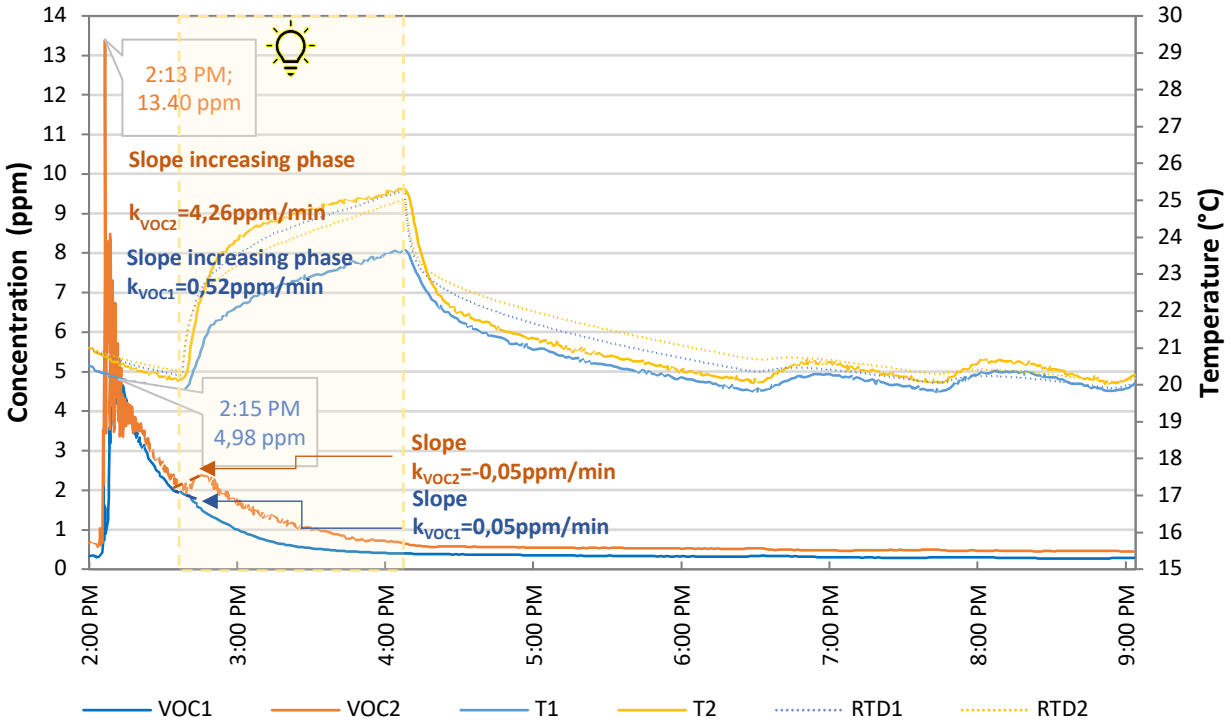

Figure 10. VOCs concentration and temperatures in the two boxes with spots load of 100 µl of MEK and TiO_2 photocatalytic activation through UV lamp. The number 1 is for box 1 (C-U) and number 2 for reference box 2 (C-L).

Figure 6 shows the desorption properties of both finishes and the influence of T change on the adsorbed VOCs with no VOCs load/sources added in the environment. As previously described in section 6.2, the increase of T was provided by irradiation (UV irradiation 3 W/m^2 and vis irradiation 18 W/m^2) with a solar lamp (300W Ultravita LUX, Osram) for 1 h, raising T from 20 °C to 28 °C. In general, data showed an increase in VOCs release under higher temperature confirming the results obtained by [14]. The increase in T increased VOCs concentration inside box 1 and box 2 of 13% (from 0.27 ppm to 0.31 ppm) and 21% (from 0.43 ppm to 0.53 ppm) after one hour of irradiation, respectively; with the L finish the increase was up to double that of C-U finish.

Moreover, after turning off the lamp in box 2 with L finish, VOCs concentration took 3 hours to return to a steady state value, 0.45 ppm instead of the initial 0.43 ppm. On the other hand, in box 1 with U finish, VOCs concentration took only 1 hour to return to a steady state value, 0.27 ppm instead of the initial 0.29 ppm.

7. Discussion

The paper concerns the evaluation of thermo-hygrometric and depolluting abilities of an innovative finish (U) in both laboratory and pilot scale tests, in comparison with a commercial one (L).

The laboratory tests demonstrated that the finish, regardless of whether commercial or innovative, had a negligible effect on thermal conductivity and water vapour permeability due to the low thickness of the layer

(few millimetres). The hygroscopic buffer capacity and depolluting abilities of the new finish improved in the same way, more than doubling the reference solution, since the two properties are linked to the high absorbing capacities of the adopted unconventional aggregates, as demonstrated also in previous works [46] [44].

The on-site tests confirmed that the innovative finish can adsorb more VOCs than a reference commercial finish even at a pilot scale. It can be explained by a different composition and by the inclusion of unconventional aggregates that affect the final structure of the mortar, resulting in higher porosity and enabling it to trap and adsorb more molecules, as reported in previously [50].

During the on-site tests, it was also demonstrated that building materials and furnishings can adsorb and desorb (re-emit) indoor air pollutants. This phenomenon is called "the sink effect" and can involve two processes: i) the adsorption (and desorption) of VOCs on a material surface, and ii) the diffusion of VOCs from the surface into the material interior. On the other hand, if the sink effect is 100% reversible, meaning that adsorbed VOCs molecules are later released, it might also lead to a protracted low-level exposure of building occupants to VOCs. Good adsorption capacity, even if irreversible, and a very low desorption rate, if reversible, are characteristics of an ideal building material for improving IAQ. This ensures that the concentration of emitted VOCs is considerably below both the perceived threshold and the IAQ requirements.

The moisture buffering ability of a finish is important [56] not only for occupants' health, but also for energy saving issues. In particular, the efficacy of moisture buffering materials is recognized for temperate zones with high humidity differences between day and night [35] [57].

The test demonstrated that environmental parameters such as T and RH modify the response of finishes in terms of adsorption/absorption of airborne pollutants, with the innovative finish more influenced by RH, whereas the commercial one more influenced by T.

Data showed an increase in VOCs release under higher T confirming the results obtained by [14]. Moreover, when RH was reduced after the high regime of 75%, the VOCs concentrations decreased in the two boxes, demonstrating the desorption of MEK from the superficial open porosity (active sites) of both finishes occurring at rising RH [58] [59]. However, between the two materials, the C-U system showed higher VOCs depolluting capacity; this was attributed both to the presence of adsorbent materials [60] and to the presence of TiO_2 in the mix-design since TiO_2 has already been proven to be able to mineralize pollutants [61].

8. Conclusions

The present work was aimed at verifying the efficacy of an innovative finish to improve IAQ in both laboratory and pilot scale tests in comparison with a commercial finish for the same applications. In particular, tests were conducted to evaluate the ability of the two finishes to passively improve indoor comfort and health in terms of thermo-hygrometric properties such as temperature and moisture buffering capacity and and depolluting abilities such as Volatile Organic Compounds (VOCs) adsorption and desorption.

From the laboratory to pilot scale results the following main conclusions can be drawn:

- Even if applied at very small thickness, the innovative finish is able to reduce the temperature peaks (about -1.5°C) better than the commercial finish at pilot scale.

- The innovative finish has a higher moisture buffering ability than the commercial finish both at lab and pilot scales.
- The indoor VOCs concentration is influenced by both T and RH and the increase of these parameters causes VOCs desorption.
- Increase of T causes VOCs desorption but at pilot scale the tested T of 25 °C does not cause the release of adsorbed VOCs from the active sites of the unconventional aggregates.
- Increase in RH causes a VOCs removal from the internal porosity of the adsorbent aggregates. For this reason, the application of the new finish in indoor environment with high RH values and RH variations, should be carefully investigated.
- Between the two finishes, the innovative one showed a higher VOCs depolluting capacity both at lab and pilot scale. This is due not only to photooxidation by TiO2 able to mineralize the pollutants if activated by UV light but also to VOCs adsorption by unconventional aggregates of the patented mix.

Patent

Italian Patent 102017000033750

Acknowledgements

The authors wish to thank to Heidelberg Materials - Italcementi, EPICO Biomasse, Evonik, and DIASEN, which kindly supplied the natural hydraulic lime, the biomass ashes, titanium dioxide, and the commercial mortar and finish. The co-grant for research contract was provided thanks to the program 'FSE-REACT-EU, PON Ricerca e Innovazione 2014-2020 DM 1062/2021'. This research activity was carried out within the MAMMUT "Malta multifunzionale a basso impatto AMbientale per il risparmio energetico, il coMfort e la salUbrità degli ambienTi di vita" Project, funded by Università Politecnica delle Marche, under the FASTER valorization program, related to the "MISE POC 2020" Announcement, CUP C36I20000130006.

References

[1] N.E. Klepeis, W.C. Nelson, W.R. Ott, J.P. Robinson, A.M. Tsang, P. Switzer, J. V Behar, S.C. Hern, W.H. Engelmann, The National Human Activity Pattern Survey (NHAPS): a resource for assessing exposure to environmental pollutants, J Expo Sci Environ Epidemiol 11 (2001) 231–252. www.nature.com/jea.

[2] United Nations Department of Economic and Social Affairs, 2023 Agenda for Sustainable Development, (n.d.). https://sdgs.un.org/goals (accessed October 26, 2024).

[3] Global Alliance for Buildings and Construction, 2020 Global status Report for Buildings and Construction. Towards a zero-emissions, efficient and resilient buildings and construction sector, 2020. www.globalabc.org.

[4] P. Wolkoff, Indoor air humidity, air quality, and health – An overview, Int J Hyg Environ Health 221 (2018) 376–390. https://doi.org/10.1016/j.ijheh.2018.01.015.

[5] Y. Al horr, M. Arif, M. Katafygiotou, A. Mazroei, A. Kaushik, E. Elsarrag, Impact of indoor environmental quality on occupant well-being and comfort: A review of the literature, International Journal of Sustainable Built Environment 5 (2016) 1–11. https://doi.org/10.1016/j.ijsbe.2016.03.006.

[6] United States Environmental Protection Agency, Indoor Air Facts No. 4 Sick Building Syndrome, Air Radiat. (6609J) Res. Dev.(MD-56) (1991) 1–4.

[7] J. González-Martín, N.J.R. Kraakman, C. Pérez, R. Lebrero, R. Muñoz, A state–of–the-art review on indoor air pollution and strategies for indoor air pollution control, Chemosphere 262 (2021) 128376. https://doi.org/10.1016/j.chemosphere.2020.128376.

[8] M. Pierpaoli, C. Giosuè, M.L. Ruello, G. Fava, Appraisal of a hybrid air cleaning process, Environmental Science and Pollution Research 24 (2017). https://doi.org/10.1007/s11356-016-7880-x.

[9] M.S. Zuraimi, R.J. Magee, D.Y. Won, G. Nong, C.D. Arsenault, W. Yang, S. So, G. Nilsson, L. Abebe, C. Alliston, Performance of sorption- and photocatalytic oxidation-based indoor passive panel technologies, Build Environ 135 (2018) 85–93. https://doi.org/10.1016/j.buildenv.2018.03.004.

[10] Q. Ren, Z. Zeng, M. Xie, Z. Jiang, Cement-based composite with humidity adsorption and formaldehyde removal functions as an indoor wall material, Constr Build Mater 247 (2020) 118610. https://doi.org/10.1016/j.conbuildmat.2020.118610.

[11] M. Bahri, H. Schleibinger, W. Render, O. Naboka, Removal performance of formaldehyde by ceiling tiles as sorptive passive panels, Build Environ 160 (2019) 106172. https://doi.org/10.1016/j.buildenv.2019.106172.

[12] Kunkel D., E. Gall, J.A. Siegel, A. Novoselac, G.C. Morrison, R.L. Corsi, Passive reduction of human exposure to indoor ozone, Build Environ 45 (2010) 445–452. https://doi.org/10.1016/j.buildenv.2009.06.024.

[13] A.D. Tran Le, J.S. Zhang, Z. Liu, D. Samri, T. Langlet, Modeling the similarity and the potential of toluene and moisture buffering capacities of hemp concrete on IAQ and thermal comfort, Build Environ 188 (2021) 107455. https://doi.org/10.1016/j.buildenv.2020.107455.

[14] J. Xiong, P. Zhang, S. Huang, Y. Zhang, Comprehensive influence of environmental factors on the emission rate of formaldehyde and VOCs in building materials: Correlation development and exposure assessment, Environ Res 151 (2016) 734–741. https://doi.org/10.1016/j.envres.2016.09.003.

[15] X. Li, L. Zhang, Z. Yang, P. Wang, Y. Yan, J. Ran, Adsorption materials for volatile organic compounds (VOCs) and the key factors for VOCs adsorption process: A review, Sep Purif Technol 235 (2020) 116213. https://doi.org/10.1016/j.seppur.2019.116213.

[16] S. Mobasser, Y. Wager, T.M. Dittrich, Indoor Air Purification of Volatile Organic Compounds (VOCs) Using Activated Carbon, Zeolite, and Organosilica Sorbents, Ind Eng Chem Res 61 (2022) 6791–6801. https://doi.org/10.1021/acs.iecr.1c04732.

[17] X. Yue, N.L. Ma, C. Sonne, R. Guan, S.S. Lam, Q. Van Le, X. Chen, Y. Yang, H. Gu, J. Rinklebe, W. Peng, Mitigation of indoor air pollution: A review of recent advances in adsorption materials and catalytic oxidation, J Hazard Mater 405 (2021) 124138. https://doi.org/10.1016/j.jhazmat.2020.124138.

[18] R. Chen, Z. Yao, N. Han, X. Ma, L. Li, S. Liu, H. Sun, S. Wang, L. Li, Insights into the Adsorption of VOCs on a Cobalt-Adeninate Metal-Organic Framework (Bio-MOF-11), ACS Omega 5 (2020) 15402–15408. https://doi.org/10.1021/acsomega.0c01504.

[19] D. Guo, D. Feng, Y. Zhang, Z. Zhang, J. Wu, Y. Zhao, S. Sun, Synergistic mechanism of biochar-nano TiO2 adsorption-photocatalytic oxidation of toluene, Fuel Processing Technology 229 (2022) 107200. https://doi.org/10.1016/j.fuproc.2022.107200.

[20] J. Jin, J.P. Kim, S. Wan, K.H. Kim, Y. Choi, P. Li, J. Kang, Z. Ma, J.H. Lee, O. Kwon, D.W. Kim, J.H. Park, Hierarchical pore enhanced adsorption and photocatalytic performance of graphene oxide/Ti-based metal-organic framework hybrid for toluene removal, Appl Catal B 317 (2022) 121751. https://doi.org/10.1016/j.apcatb.2022.121751.

[21] J.D. Bersch, I. Flores-Colen, A.B. Masuero, D.C.C. Dal Molin, Photocatalytic TiO2-Based Coatings for Mortars on Facades: A Review of Efficiency, Durability, and Sustainability, Buildings 13 (2023) 186. https://doi.org/10.3390/buildings13010186.

[22] J. Yu, X. Wang, L. Chen, G. Lu, G. Shi, X. Xie, Y. Wang, J. Sun, Enhanced adsorption and visible-light photocatalytic degradation of toluene by CQDs/UiO-66 MOG with hierarchical pores, Chemical Engineering Journal 435 (2022) 135033. https://doi.org/10.1016/j.cej.2022.135033.

[23] C. Giosuè, Q.L. Yu, M.L. Ruello, F. Tittarelli, H.J.H. Brouwers, Effect of pore structure on the performance of photocatalytic lightweight lime-based finishing mortar, Constr Build Mater 171 (2018). https://doi.org/10.1016/j.conbuildmat.2018.03.106.

[24] R. Sugrañez, J.I. Álvarez, M. Cruz-yusta, I. Mármol, J. Morales, J. Vila, L. Sánchez, Enhanced photocatalytic degradation of NOx gases by regulating the microstructure of mortar cement modified with titanium dioxide, Build Environ 69 (2013) 55–63. https://doi.org/10.1016/j.buildenv.2013.07.014.

[25] I. Karatasios, M.S. Katsiotis, V. Likodimos, A.I. Kontos, G. Papavassiliou, P. Falaras, V. Kilikoglou, Photo-induced carbonation of lime-TiO2 mortars, Appl Catal B 95 (2010) 78–86. https://doi.org/10.1016/j.apcatb.2009.12.011.

[26] S.S. Lucas, V.M. Ferreira, J.L.B. De Aguiar, Incorporation of titanium dioxide nanoparticles in mortars — Influence of microstructure in the hardened state properties and photocatalytic activity, Cem Concr Res 43 (2013) 112–120. https://doi.org/10.1016/j.cemconres.2012.09.007.

[27] Q.L. Yu, M.M. Ballari, H.J.H. Brouwers, Indoor air purification using heterogeneous photocatalytic oxidation. Part II: Kinetic study, Appl Catal B 99 (2010) 58–65. https://doi.org/10.1016/j.apcatb.2010.05.032.

[28] A.L. Velosa, P.B. Cachim, Hydraulic-lime based concrete: Strength development using a pozzolanic addition and different curing conditions, Constr Build Mater 23 (2009) 2107–2111. https://doi.org/10.1016/j.conbuildmat.2008.08.013.

[29] G. Cultrone, E. Sebastián, M.O. Huertas, Forced and natural carbonation of lime-based mortars with and without additives: Mineralogical and textural changes, Cem Concr Res 35 (2005) 2278–2289. https://doi.org/10.1016/j.cemconres.2004.12.012.

[30] J. Torkaman, A. Ashori, A. Sadr Momtazi, Using wood fiber waste, rice husk ash, and limestone powder waste as cement replacement materials for lightweight concrete blocks, Constr Build Mater 50 (2014) 432–436. https://doi.org/10.1016/j.conbuildmat.2013.09.044.

[31] F. Tittarelli, C. Giosuè, A. Mobili, Recycled Glass as Aggregate for Architectural Mortars, Int J Concr Struct Mater 12 (2018) 1–11. https://doi.org/10.1186/s40069-018-0290-3.

[32] C. Fan, R. Huang, H. Hwang, S. Chao, Properties of concrete incorporating fine recycled aggregates from crushed concrete wastes, Constr Build Mater 112 (2016) 708–715. https://doi.org/10.1016/j.conbuildmat.2016.02.154.

[33] B.S. Thomas, J. Yang, K.H. Mo, J.A. Abdalla, R.A. Hawileh, E. Ariyachandra, Biomass ashes from agricultural wastes as supplementary cementitious materials or aggregate replacement in cement/geopolymer concrete: A comprehensive review, Journal of Building Engineering 40 (2021). https://doi.org/10.1016/j.jobe.2021.102332.

[34] B.K. Kreiger, W. V. Srubar, Moisture buffering in buildings: A review of experimental and numerical methods, Energy Build 202 (2019) 109394. https://doi.org/10.1016/j.enbuild.2019.109394.

[35] M. Zhang, M. Qin, C. Rode, Z. Chen, Moisture buffering phenomenon and its impact on building energy consumption, Appl Therm Eng 124 (2017) 337–345. https://doi.org/10.1016/j.applthermaleng.2017.05.173.

[36] C. Liu, Y. Zhang, L. Sun, W. Gao, X. Jing, W. Ye, Influence of indoor air temperature and relative humidity on learning performance of undergraduates, Case Studies in Thermal Engineering 28 (2021) 101458. https://doi.org/10.1016/j.csite.2021.101458.

[37] M.I. Gomes, J. Lima, T. Santos, J. Gomes, P. Faria, The Benefits of Eco-efficient Plasters for Occupant's Health-A Case Study, in: Ecological and Health Effects of Building Materials, Springer, Cham, 2022. https://doi.org/https://doi.org/10.1007/978-3-030-76073-1_20.

[38] Z. Shayegan, M. Bahri, F. Haghighat, A review on an emerging solution to improve indoor air quality: Application of passive removal materials, Build Environ 219 (2022) 109228. https://doi.org/10.1016/j.buildenv.2022.109228.

[39] J. Auvinen, L. Wirtanen, The influence of photocatalytic interior paints on indoor air quality, Atmos Environ 42 (2008) 4101–4112. https://doi.org/10.1016/j.atmosenv.2008.01.031.

[40] M.V. Diamanti, R. Paolini, M. Rossini, A.B. Aslan, M. Zinzi, T. Poli, M.P. Pedeferri, Long term self-cleaning and photocatalytic performance of anatase added mortars exposed to the urban environment, Constr Build Mater 96 (2015) 270–278. https://doi.org/10.1016/j.conbuildmat.2015.08.028.

[41] M.S. Vega-Mendoza, E. Luévano-Hipólito, L.M. Torres-Martínez, Design and fabrication of photocatalytic coatings with α/β-Bi2O3 and recycled-fly ash for environmental remediation and solar fuel generation, Ceram Int 47 (2021) 26907–26918. https://doi.org/10.1016/j.ceramint.2021.06.100.

[42] J. Jeon, J.H. Park, S. Wi, B.Y. Yun, T. Kim, S. Kim, Field study on the improvement of indoor air quality with toluene adsorption finishing materials in an urban residential apartment, Environmental Pollution 261 (2020) 114137. https://doi.org/10.1016/j.envpol.2020.114137.

[43] A. Nieto-Márquez, M. de Mateo, A. Barrios, M. del M. de la F. García-Soto, A. Narros, Improving indoor air quality by using photocatalytic paints. Real scale study at the Technical University of Madrid, Atmos Pollut Res 14 (2023) 101827. https://doi.org/10.1016/j.apr.2023.101827.

[44] C. Giosuè, M. Pierpaoli, C. di Perna, B. Citterio, G. Mangiaterra, M.L. Ruello, F. Tittarelli, Properties of an innovative multi-functional finish for the improvement of indoor air quality, Build Environ 233 (2023) 110091. https://doi.org/10.1016/j.buildenv.2023.110091.

[45] C. Giosuè, M. Pierpaoli, A. Mobili, M.L. Ruello, F. Tittarelli, Multifunctional Lightweight Mortars for Indoor Applications to Improve Comfort and Health of Occupants: Thermal Properties and Photocatalytic Efficiency, Front Mater 7 (2020) 1–10. https://doi.org/10.3389/fmats.2020.00255.

[46] Q. Maqbool, N. Czerwinska, C. Giosue, S. Sabbatini, M.L. Ruello, F. Tittarelli, New waste-derived TiO2 nanoparticles as a potential photocatalytic additive for lime based indoor finishings, J Clean Prod 373 (2022) 133853. https://doi.org/10.1016/j.jclepro.2022.133853.

[47] E. Boonen, A. Beeldens, Photocatalytic roads: From lab tests to real scale applications, European Transport Research Review 5 (2013) 79–89. https://doi.org/10.1007/s12544-012-0085-6.

[48] G.E. Imoberdorf, H.A. Irazoqui, O.M. Alfano, A.E. Cassano, Scaling-up from first principles of a photocatalytic reactor for air pollution remediation, Chem Eng Sci 62 (2007) 793–804. https://doi.org/10.1016/j.ces.2006.10.004.

[49] N.M.M. Ramos, J.M.P.Q. Delgado, V.P. De Freitas, Influence of finishing coatings on hygroscopic moisture buffering in building elements, Constr Build Mater 24 (2010) 2590–2597. https://doi.org/10.1016/j.conbuildmat.2010.05.017.

[50] C. Shi, H. Zhang, Y. Xuan, Experimental investigation of thermal properties and moisture buffering performance of composite interior finishing materials under different airflow conditions, Build Environ 160 (2019) 106175. https://doi.org/10.1016/j.buildenv.2019.106175.

[51] N. Pétigny, J. Zhang, E. Horner, S. Steady, M. Chenal, G. Mialon, V. Goletto, Indoor air depolluting material: Combining sorption testing and modeling to predict product's service life in real conditions, Build Environ 202 (2021) 107838. https://doi.org/10.1016/j.buildenv.2021.107838.

[52] C. Giosuè, A. Mobili, G. Toscano, M.L. Ruello, F. Tittarelli, Effect of Biomass Waste Materials as Unconventional Aggregates in Multifunctional Mortars for Indoor Application, Procedia Eng 161 (2016) 655–659. https://doi.org/10.1016/j.proeng.2016.08.724.

[53] C. Rode, R. Peuhkuri, L.H. Mortensen, K.K. Hansen, B. Time, A. Gustavsen, T. Ojanen, J. Ahonen, K. Svennberg, J. Arfvidsson, Moisture buffering of building materials, BYG DTU Report, Technical University of Denmark, 2005. http://www.byg.dtu.dk/upload/institutter/byg/publications/rapporter/byg-r126.pdf.

[54] F. Tittarelli, C. Giosuè, A. Mobili, M.L. Ruello, Influence of binders and aggregates on VOCs adsorption and moisture buffering activity of mortars for indoor applications, Cem Concr Compos 57 (2015) 75–83. https://doi.org/10.1016/j.cemconcomp.2014.11.013.

[55] C. Giosuè, M. Pierpaoli, A. Mobili, M.L. Ruello, F. Tittarelli, Influence of Binders and Lightweight Aggregates on the Properties of Cementitious Mortars: From Traditional Requirements to Indoor Air Quality Improvement, Materials 10 (2017) 978. https://doi.org/10.3390/ma10080978.

[56] H.J. Kim, S.S. Kim, Y.G. Lee, K.D. Song, The hygric performances of moisture adsorbing/desorbing building materials, Aerosol Air Qual Res 10 (2010) 625–634. https://doi.org/10.4209/aaqr.2010.08.0070.

[57] V. Cascione, D. Maskell, A. Shea, P. Walker, M. Mani, Comparison of moisture buffering properties of plasters in full scale simulations and laboratory testing, Constr Build Mater 252 (2020) 119033. https://doi.org/10.1016/j.conbuildmat.2020.119033.

[58] C. Jung, N.S.A. Mahmoud, N. Alqassimi, Identifying the relationship between VOCs emission and temperature/humidity changes in new apartments in the hot desert climate, Front Built Environ 8 (2022) 1018395. https://doi.org/10.3389/fbuil.2022.1018395.

[59] P. Markowicz, L. Larsson, Influence of relative humidity on VOC concentrations in indoor air, Environmental Science and Pollution Research 22 (2015) 5772–5779. https://doi.org/10.1007/s11356-014-3678-x.

[60] X. Zhou, Y. Liu, C. Song, X. Wang, F. Wang, J. Liu, Modelling and testing of VOC source suppression effect of building materials modified with adsorbents, Build Environ 154 (2019) 122–131. https://doi.org/10.1016/j.buildenv.2019.03.003.

[61] K.W. Shah, W. Li, A review on catalytic nanomaterials for volatile organic compounds VOC removal and their applications for healthy buildings, Nanomaterials 9 (2019) 910. https://doi.org/10.3390/nano9060910.